Proceedings World Geothermal Congress 2026
Calgary, Canada, June 8 – 11, 2026

Assessing the thermal impacts of an HT-ATES system on groundwater resources for varying hydrogeological conditions

Stijn Beernink[1,2]*, Philip J. Vardon[2], Martin Bloemendal[2,3], Niels Hartog[1,4]

[1]KWR Water Research, [2]Delft University of Technology, [3]TNO Dutch Geological Survey, [4]Utrecht University

*stijn.beernink@kwrwater.nl

Keywords: HT-ATES, groundwater resources, thermal impact, recovery efficiency

1. INTRODUCTION

Aquifer Thermal Energy Storage (ATES) is seen as a key enabling technology to overcome the seasonal mismatch between availability of sustainable heat in summer and heat demand in winter. These systems use a doublet of tube wells to store and recover heated groundwater at storage temperatures ranging between approximately 15 to 100 °C in aquifers that usually have low ambient temperatures (e.g. 10 to 15 °C). At storage temperatures above 50 °C ATES systems are generally considered to be 'High Temperature' systems (HT-ATES). Although in the design of HT-ATES systems the aim is to recover as much of the stored heat as possible, high-performing wells still lose 10 to 30% of the stored heat to the subsurface each year, resulting in increasing subsurface temperatures in the vicinity of the wells, potentially impacting groundwater resources depending on the type and characteristics of local (horizontal and vertical) neighboring underground formations. Previous studies provide generic insight in what processes affect heat losses during storage, and how to minimize these losses (Beernink et al., 2024; Doughty et al., 1982; Sheldon et al., 2021). However, until now only little attention has been given to the potential (negative) thermal impacts of these heat losses. Therefore, in this study the sensitivity of the hydrogeological properties of the top sealing layer of a HT-ATES well on thermal impact to overlying layers is assessed. To this end, a hydro-thermal numerical model is used to simulate the transport and distribution of the stored heat in time. The subsurface conditions are based on a recent drilling and characterization efforts done to design an actual HT-ATES pilot system at the Technical University of Delft, The Netherlands, and are varied in order to test the sensitivity to hydrogeological conditions.

2. METHODS

2.1. Description of subsurface characterization in Delft

In 2021, a test drilling was carried out in Delft (The Netherlands) to assess the suitability of the shallow subsurface (0 - 500m depth) for seasonally storing renewable heat from a geothermal well on the campus of Delft University of Technology with HT-ATES. The results of this test drilling were described in Vardon et al. (2022) and two suitable aquifers were identified by Beernink et al. (2025). The sealing clayey/silty layer above the deepest aquifer, this aquifer was assessed to be most suitable for HT-ATES because of its large flow capacity per well, showed heterogeneity and uncertain properties (Figure 1). Based on the expected operational conditions in Delft (injection temperature of 80 °C, constant flow rate of 3,333 m^3/d, 150 days of injection, 150 days of recovery) the simulated recovery efficiency in the fifth year was 75% (Beernink et al., 2025).

In this study the boundary conditions and inputs determined by Beernink et al. (2025) are used and build upon to further assess the impact of varying properties of the sealing layer overlying the storage aquifer on the recovery efficiency and thermal impact of the stored heat.

2.2. Numerical simulations and varied hydrogeological properties of sealing layer

Numerical simulations of a single HT-ATES well were done with the SEAWATv4 model (Langevin et al., 2007) in python using Flopy (Bakker et al., 2016). An axisymmetric grid was used and therefore radial symmetry was assumed, similar to Beernink et al. (2024). Different layers with varying hydrogeological and thermal properties were used of lateral homogeneous and isotropic properties following Beernink et al. (2025). The hydraulic conductivity was assumed to be anisotropic with anisotropy ratio (K_h/K_v) of 5 in all layers.

In the defined base case hydrogeological model the sealing layer between -77 to -123m depth consists of two very silty layers with horizontal hydraulic conductivity of 1 m/d intersected by a permeable fine sandy layer (10 m/d) between -100 to -110m below surface level (Figure 1A). To assess the impact of varying hydrogeological properties, the thickness and continuity of the sealing layer above (and thus the hydraulic resistance) is varied:

- Base case: Two very silty layers above intersected by sandy layer between -100 to -110m (Figure 1)

- Min sealing layer: Low hydraulic resistance: 5m very silty layer above storage aquifer from -118 to -123m
- Max sealing layer: High hydraulic resistance: Full sealing layer: thick very silty layer between -76 to -123m

2.3. Assessment framework for thermal impacts

Thermal impacts are assessed following two approaches:

1. Monitoring the total energy increase per layer. In the simulation model, the energy that is stored in the different aquifer layers is monitored. This is presented here as the energy in three sections: the total energy in the storage aquifer, the total energy in the layers above the storage aquifer (overlying layers, Figure 1A) and the total energy in the layers below the storage aquifer (underlying layers, Figure 1A).

2. Development in time of temperature contours. The development in time of the maximum distance of the temperature increase contours (+5°C, +15°C and +40°C compared to ambient 10 °C) is monitored in the simulation. This is done both radially in the storage aquifer and vertically above and below the storage aquifer.

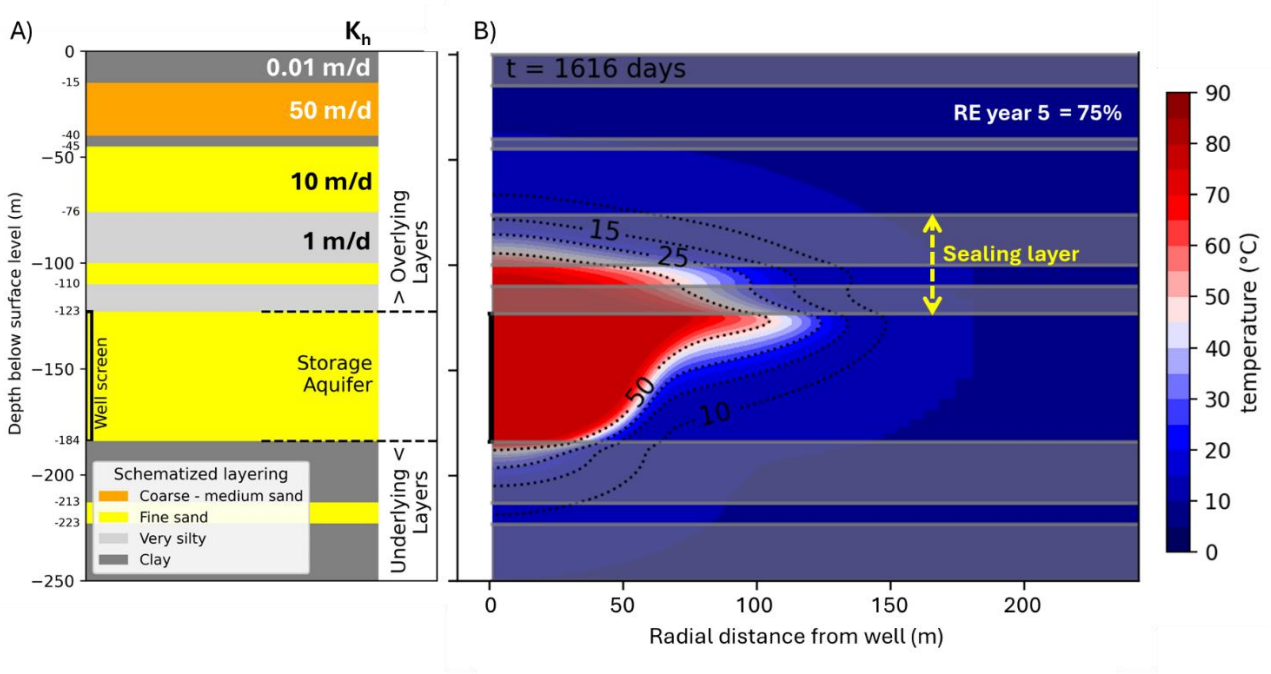

Figure 1. A) The hydrogeological base case model based on a test drilling in Delft. Indicated are the location of the well screen and the hydraulic conductivity (K_h) of the 4 different layers. Also, the model is dissected into three different zones: the storage aquifer, the overlying layers (0 to – 123m depth) and the underlying layers (-184 to -250m). B) Cross section of the temperature distribution in the subsurface after full loading of the aquifer in the fifth year of operation. The two very silty layers overlying the storage aquifer are identified as the sealing layer. Adapted from Beernink et al. (2025) .

3. RESULTS

For the base case scenario, initially (during the first months) the total energy stored in the subsurface with the HT-ATES well is almost entirely situated in the storage aquifer itself, and as heat losses each cycle continue, the total energy stored in the storage aquifer increases, but the rate of increase reduces (Figure 2A). Almost all of the energy that is stored in the subsurface, which is not contained in the storage aquifer, is distributed in time to the overlying layers above the storage aquifer and almost none is lost to the deeper layers. Due to buoyancy-driven flow in the storage aquifer, thermal energy is transported upwards and ambient (cold) groundwater is transported to the bottom of the aquifer. As a result, high temperatures are present at the top of the aquifer leading to relatively large heat losses to the overlying layers above the storage aquifer (here >20 times more heat lost to the overlying compared to underlaying layers). In addition, more heat is transported into the top sealing layer compared to the bottom sealing layer during injection because the hydraulic conductivity of the top sealing layer is higher and hence also some advection into this layer occurs.

For the tested scenarios of the sealing layer, the recovery efficiency decreases slightly (72% in 5th year) for the case with the lowest hydraulic resistance (Min sealing layer) compared to the base case and the case with highest hydraulic resistance (both 75% in the fifth year). Although slightly more heat is lost to the subsurface, the amount of heat that is stored in the storage aquifer over time actually decreases for the case with lowest hydraulic resistance (Figure 2B). Hence, more of the lost heat is distributed towards the layers above the storage aquifer (overlying layers) for the situation with low hydraulic resistance (Min sealing layer, Figure 2C). With highest hydraulic resistance of the sealing layer, the heat that is stored in the subsurface is distributed slightly more in the aquifer (Figure 2B) and less into the overlying layers (Figure 2C) at equal recovery efficiency compared to the base case scenario.

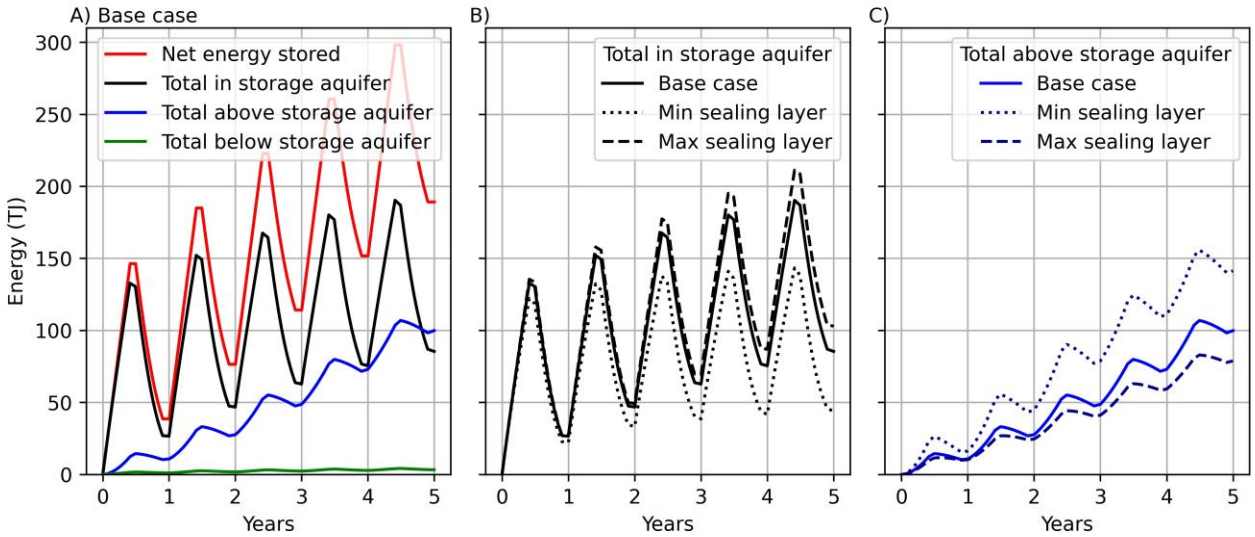

Figure 2 Simulation results of heat distribution monitoring in the subsurface over time. A) the base case scenario from Beernink et al. (2025) – in prep. B) total energy in the storage aquifer for varying sealing layer properties and C) total energy above the storage aquifer for varying sealing layer properties.

Over time, the maximum radial distances of the +5 °C, +15 °C and +40 °C contours in the storage aquifer for the base case scenario (at the top of the aquifer, Figure 1B) are already observed at further distance from the well than the theoretical thermal radius (no heat transfer) in the first year (Figure 3A.I). Over the years, the distance of these temperature contours from the well increase further because more heat is lost each year and transported to the top of the aquifer. Moreover, the width of the mixed front and hence the distance between the temperature contours increases further mainly because of conduction (Figure 3A.I). Nevertheless, after the first 3 years the radial distance from the well of the +5 °C, +15 °C and +40 °C temperature contours seem to stabilize. Vertically, the maximal distance of the temperature contours for the base case scenario in the first 2 years is decreased during extraction, indicating that heat transport to the layers above is influenced partly by advection of the heat in and out the overburden (Figure 3B.I). Moreover, as the heat protrudes further into the layers above the storage aquifer (e.g. years 3-5), the upward speed of the temperature contours decrease, especially for the +40 °C temperature contour.

The effect of varying hydraulic resistance on the distance of the +40 °C contour, both radially from the well and vertically into the overlying layers is analyzed for the two tested scenarios with lower (min) and higher (max) sealing layer hydraulic resistance and compared to the base case (Figure 3A.II and Figure 3B.II). For the base case scenario and the scenario with highest hydraulic resistance, the radial speed into the aquifer of the +40 °C contour is similar and reduces over the years but is not stabilized after 5 years (Figure 3A.II). Vertically, the +40 °C contour protrudes less far into the sealing layer above for the scenario with highest hydraulic resistance compared to the base case scenario, likely because less of the hot water is injected in the sealing layer due to advection and also because convection (buoyancy-driven flow) occurs in the base case scenario in the highly permeable layer between -110 and -120m depth. For the case with low hydraulic resistance, the relatively thin sealing layer (5m) is heated rather quickly (+40 °C after 3 months of injection) resulting in buoyancy-driven flow in the permeable sand layer above leading to relatively fast transport (30m/y between year 1 and year 2) of the high temperature heat to the top of the above lying sandy layer resulting after 2.5 years in upward transport of the +40 °C contour of more than 70m (Figure 3B.II). There, the clay layer at 45m depth (Figure 1) is reached and the upward movement of the heat is again slowed down. Hence, convection in permeable layers above the

storage aquifer has the potential to quickly transport high temperature heat upwards to overlying layers compared to when impermeable layers are heated.

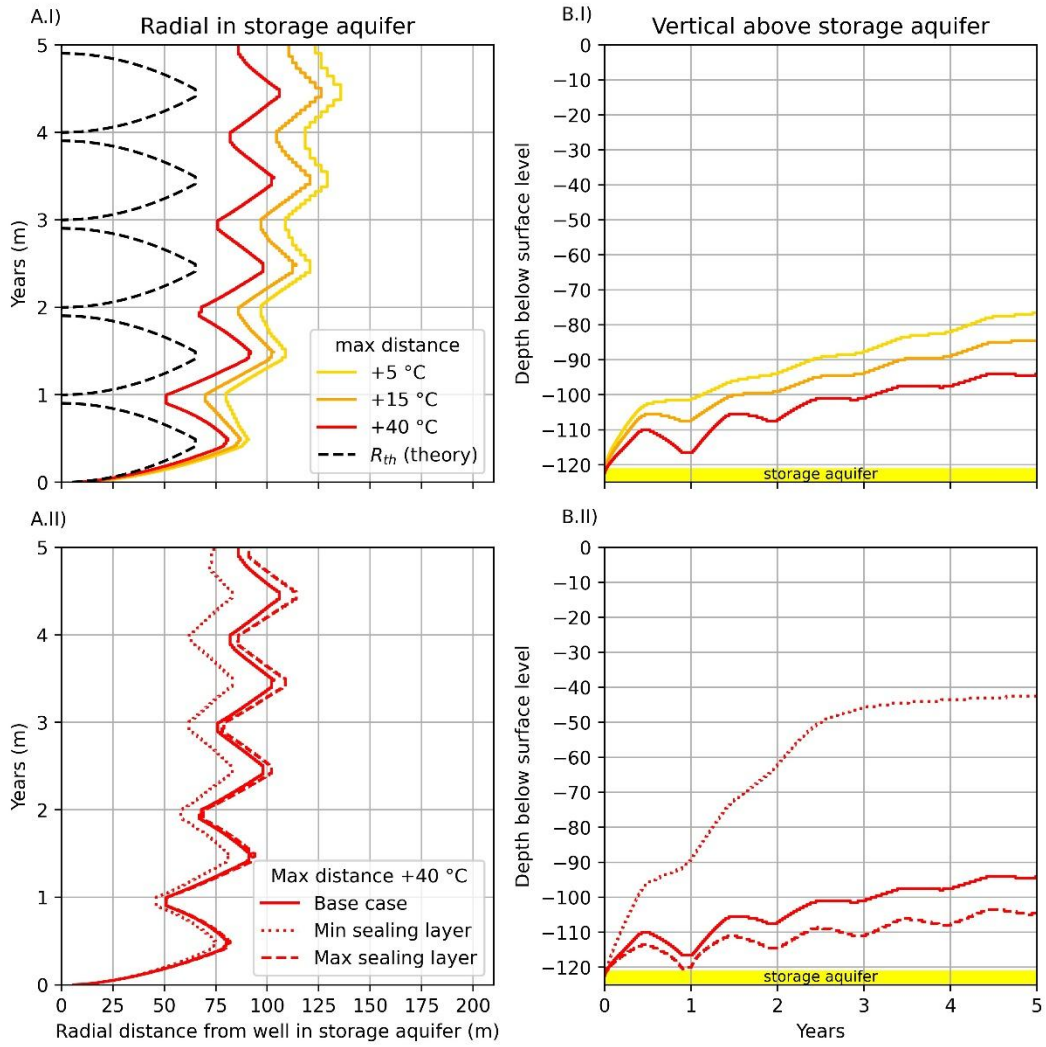

Figure 3 Distribution of the temperature contours in time. A.I) For the base case, the maximum radial distance from the well in the storage aquifer of the +5, +15 and +40 °C compared to the theoretical thermal radius and B.I) the maximum vertical distance from the top of the storage aquifer into the layers above the storage aquifer (top at -123m) of the +5, +15 and +40 °C contours in time. Effect of varying hydraulic resistance of the sealing layer above the storage aquifer on A.II) the +40 °C radial temperature contour in the storage aquifer and B.II) vertically into the overlying layers.

4. DISCUSSION

For the hydrogeological conditions in this study, the simulations show that thermal energy is transported into the sealing layer above the storage aquifer by heat conduction from the hot plume in the top of the aquifer but also due to advection from the storage aquifer into the sealing layer during injection (mainly close to the well). The vertical resistance of the sealing very silty layer above the storage aquifer is determined by the thickness of the silty layers, and also by the vertical hydraulic conductivity of the silty layers. In this case, the anisotropy ratio of the vertical to the horizontal hydraulic conductivity was assumed to be a factor 5, meaning that the K_v of the silty layers was 0.2 m/d (Figure 1). Determining the vertical hydraulic conductivity is difficult in practice and therefore this value is relatively uncertain and is influenced by the existence and continuity of impermeable layers (like clay) in the mostly silty layers. The thermal properties of the chosen layers is based on thermal conductivity measurements of plugs on the cm-scale. Although the range of these values is rather small (+/- 20%), the upscaling of these values could imply some uncertainty that is not assessed in this study.

In the simulation, ambient groundwater flow is not included as the expected flow rates in the storage aquifer in Delft is expected to be rather low (<5m/year). Hence, not much effect is expected on the recovery efficiency of the well (Bloemendal & Hartog, 2018). However, the thermal impact in the layers above the storage aquifer could be impacted by groundwater flow, but for which conditions this is important, is at this point unknown and is not taken into account in these simulations.

5. CONCLUSIONS

In this study, the thermal impact of thermal energy storage with HT-ATES is assessed for a case-study in Delft. Two metrics are used to assess the thermal impact developing over time: the distribution of thermal energy increase in the different layers of the subsurface and the distance of the +5, +15 and +40 °C temperature increase contours from the well (radial) and the storage aquifer (vertical). With the HT-ATES well, 150 TJ of heat is seasonally stored at 80 °C and simulated for five years, resulting in an average recovery efficiency of 75% for the base case scenario. For the hydrogeological conditions of the base case scenario, the thermal energy that is not recovered is distributed mainly into the top of the storage aquifer due to buoyancy-driven flow in the storage aquifer leading to high losses to overlying layers. These heat losses to overlying layers slightly increase over the 5 simulated years. Varying the hydraulic resistance of the sealing layer above the storage aquifer only slightly influenced the recovery efficiency, but led to distinct differences in the observed thermal impact. Quick breakthrough and acceleration of temperature increase towards overlying layers are observed for the situation with only a limited hydraulic resistance of the sealing layer above the storage aquifer leading to convection in permeable layers above the storage aquifer and increased vertical transport. Hence, the vertical proximity of permeable layers overlying the storage aquifer have a strong impact on the thermal effects that are to be expected by HT-ATES wells.

Acknowledgements

This research was supported by the Dutch project WarmingUP-GOO and the European project PUSH-IT. The WarmingUP-GOO project is funded in the MMIP program of RVO (TSE-19-07-08) in the Netherlands. PUSH-IT is funded in the HORIZON Europe program with grant agreement ID: 101096566.

References

Bakker, M., Post, V., Langevin, C. D., Hughes, J. D., White, J. T., Starn, J. J., & Fienen, M. N. (2016). Scripting MODFLOW model development using Python and FloPy. *Groundwater, 54*(5), 733-739. doi:10.1111/gwat.12413

Beernink, S., Bloemendal, M., Hartog, N., & Vardon, P. J. (2025). *Characterizing the subsurface for HT-ATES well design and thermal impact analysis: a case study*. Paper presented at the European Geothermal Congres, Zürich.

Beernink, S., Hartog, N., Vardon, P. J., & Bloemendal, M. (2024). Heat losses in ATES systems: The impact of processes, storage geometry and temperature. *Geothermics, 117*, 102889. doi:https://doi.org/10.1016/j.geothermics.2023.102889

Bloemendal, M., & Hartog, N. (2018). Analysis of the impact of storage conditions on the thermal recovery efficiency of low-temperature ATES systems. *Geothermics, 17*, 306-319. doi:10.1016/j.geothermics.2017.10.009

Doughty, C., Hellström, G., & Fu Tsang, C. (1982). A Dimensionless parameter Approach to the Thermal Behavior of an Aquifer Thermal Energy Storage System. *Water Resources Research, 18*(3), 571-578. doi:10.1029/WR018i003p00571

Langevin, C. D., Thorne, D. T., Dausman, A. M., Sukop, M. C., & Guo, W. (2007). SEAWAT version 4: a computer program for simulation of multi-species solute and heat transport. In U.S.G.S. (Ed.), *Techniques and Methods, book 6*. Reston, Virginia, USA.

Sheldon, H. A., Wilkins, A., & Green, C. P. (2021). Recovery efficiency in high-temperature aquifer thermal energy storage systems. *Geothermics, 96*, 1-18. doi:10.1016/j.geothermics.2021.102173

Vardon, P. J., Laumann, S., Schmiedel, T., Vargas Meleza, L., Barnhoorn, A., Abels, H., . . . van den Berg, J. (2022). *Drilling report: Delftse Hout multipurpose research borehole. DAPGEO-02*. Retrieved from Delft: